Permafrost, Phillips, Springman & Arenson (eds)
© 2003 Swets & Zeitlinger, Lisse, ISBN 90 5809 582 7

Permafrost evolution under the influence of long-term climate fluctuations and glacio-eustatic sea-level variation: region of Laptev and East Siberian Seas, Russia

N.N. Romanovskii
Moscow State University, Moscow, Russia

H.-W. Hubberten
Alfred Wegener Institute for Polar and Marine Research, Potsdam, Germany

V.E. Romanovsky
University of Alaska, Fairbanks, USA

A.L. Kholodov
Institute of Physical–Chemical & Biological Problem of Soil Science RAS, Pushchino, Russia

ABSTRACT: Results of a five-year investigation of permafrost and gas-hydrate stability zone evolution on the Laptev and East Siberia Seas shelf are presented. For investigation of permafrost and gas hydrate stability zone (GHSZ) evolution during the Middle Pleistocene–Holocene (last 400 ka), a palaeo-geographic scenario and numerical model were developed. The model takes into consideration the duration of permafrost agradation and degradation, existence of permafrost temperature zonality, different geological composition and geothermal heat flux in different geological structures etc. Based on the modelling the following conclusions can be made. Both offshore permafrost and GHSZ recently exist from the shoreline till to the upper part of continental slope. Delay of the maximal permafrost thickness relative to the climatic extremes and different evolution of offshore permafrost thickness and GHSZ at different seawater depths is shown.

1 INTRODUCTION

The study area includes the 1000-km wide shelf of the Laptev Sea and the western part of the East Siberian Sea and aggradational coastal plains bounded by mountains from the south (Fig.1).

This territory has never been extensively glaciated (Sher, 2000). Sea-level fluctuations in the Late Cenozoic period were therefore mainly of a glacio-eustatic nature. Neotectonic movements were dominated by subsidence accompanied by sediment accumulation. The geological structure of this territory is extremely complex; with tectonic structures of different ages, including several rift zones (Tectonic Map, 1998; Drachev *et al.*, 1995). Based on data extrapolated from shelf rifts within the continent, the offshore rift zones are characterized by high variations in the geothermal heat flux ($\mathbf{q_{gt}}$) values. In the Mom and Baikal rift zones (Balobaev, 1991; Lysak, 1988) therefore, $\mathbf{q_{gt}}$ values vary from 40 to 70 mW/m^2 in relatively undisturbed blocks, and exceed 100 mW/m^2 in fault zones.

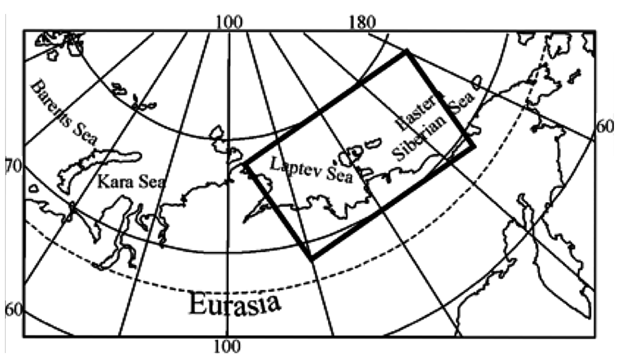

Figure 1. Scheme of the study area location.

The coastal plains and islands are characterised by the presence of continuous permafrost with a thickness of 300–400 m in the south to 500–600 m in the north (Geocryology of the USSR, 1988). The archipelago of the New Siberian Islands separates the Laptev and East Siberian seas. The zonality of permafrost mean annual ground temperature ($\mathbf{t_{ma}}$) is quite distinct within the coastal lowlands and islands. The gradient $\mathbf{t_{ma}}$ reaches 1.5°C per 1° latitude.

The mean annual bottom temperature of seawater and surficial sediments ($\mathbf{t_{sf}}$) in these seas varies from -0.5 to -2.0°C (Dmtrienko *et al.*, 2001). This creates relatively uniform temperature conditions at the shelf surface and favours the preservation of relic offshore permafrost.

Up to the mid-1990s, data on the relic offshore permafrost and subsea taliks was rather fragmentary. This data were summarised by Gavrilov *et al.* (2001). In recent years, wide-scale investigations of offshore permafrost have been performed within the framework of joint Russian–German projects "Laptev Sea System" and "System Laptev Sea 2000." Modern concepts of permafrost conditions in the studied region are outlined in the paper by Hubberten and

Romanovskii published in this volume (Hubberten & Romanovskii, 2003).

The aim of this paper is to discuss the problem of permafrost evolution under the impact of climate changes and glacial-eustatic regressive–transgressive cycles on the Arctic sea shelf of the eastern part of Siberia.

2 FORMULATION OF THE PROBLEM

The appearance of terrestrial permafrost in the north-east of Eurasia dates back to the end of the Pliocene. Since that time, terrestrial permafrost has been subjected to several cycles of thawing from the surface, probably causing a decrease in its thickness. The offshore permafrost within the shelf is thought to have developed after the Karginskaya transgression, as a result of shelf exposure and freezing in the Sartan cryochron, i.e., about 24–18 ka BP. Afterwards, it partially degraded during the latest transgression (see for example Solov'ev, 1981; Fartyshev, 1993; Danilov, 2000). For this study, the primary objectives were to characterise the evolution of the ice-bonded permafrost on the shelf, assess its probable thickness in the modern epoch and to study permafrost evolution affected by climate change and changes in relative sea level. These objectives were met by developing a permafrost evolution model and a set of climate scenarios, which were used to provide boundary conditions to the model. Initially, while simulating the development of offshore permafrost, the authors assumed that it had appeared after the Kazantsevskay transgression, after 100 ka BP (Romanovskii *et al.,* 1998). Later, we developed a palaeo-geographic scenario of permafrost evolution in the region within the last 400 ky, i.e., within four climatic and glacio-eustatic cycles (Kholodov *et al*., 2000).

3 BOUNDARY CONDITIONS AND ASSUMPTIONS ACCEPTED IN THE MODELS OF PERMAFROST EVOLUTION

In order to develop an appropriate palaeo-geographic scenario of permafrost evolution during four climatic and glacio-eustatic cycles, we used the climatic (palaeo-temperature) curve derived from the Vostok ice core in Antarctica (Petit *et al.*, 1999) and the results of palaeo-reconstructions obtained by different methods for the Quaternary sediments of coastal lowlands and Arctic islands. These results were summarised by the authors (Gavrilov & Tumskoy, 2000; Romanovskii & Hubberten, 2001). The general trend of temperature change and their periodicity were taken from the Antarctic palaeo-temperature curve (Gavrilov *et al*., 2000). Regional palaeo-reconstructions for dated extreme climatic events were used to assess the amplitude of changes (relative to the modern state) in permafrost conditions at certain latitudes. Various indicators of palaeo-cryogenic conditions were used. For instance, the presence of features of long-term thawing of the deposits indicated the rise of mean annual ground temperatures – $\mathbf{t_{ma}}$ above 0°C during warm climatic phases (Kholodov *et al*., 2000). Cold climatic events were judged from the presence of polygonal ice wedges in different kinds of sediments, which made it possible to assess the ranges of $\mathbf{t_{ma}}$ lowering (Garilov & Tumskoy, 2000).

It was assumed that the terrestrial permafrost $\mathbf{t_{ma}}$ zonality in the past corresponded to the modern permafrost temperature zonality. The shelf surface topography in the past was also assumed to be the same as in the modern epoch. A near-bottom seawater temperature equal to the mean annual temperature of bottom sediments $\mathbf{t_{sf}}$ (Zigarev, 1997) was taken equal to −1.8°C for the periods of transgression, and the freezing temperature of bottom sediments and continental deposits was taken equal to −2.0°C. A set of palaeo-temperature curves (for both $\mathbf{t_{ma}}$ and $\mathbf{t_{sf}}$) were developed for a range of latitudes from 70 to 78° north and for different sea depths. The sea level fluctuations were assumed to be of a glacio-eustatic nature. They were adapted for modelling from glacial-eustatic curves developed by various authors for different time periods. The glacio-eustatic curve for a period from 400 to 120 ky BP was taken from Petit *et al*. (1999), the curve for the period from 120 to 20 ky BP, from Chappel *et al*. (1996), and the curve for the period from 20 ka BP to the recent time, from Fairbanks (1989). The latter curve was verified for the Laptev Sea region by comparison with sea level history based on sedimentary deposits (Bauch *et al.*, 2002). The scenario adapted for the modelling assumed that, starting from the shelf submergence, the mean annual temperature $\mathbf{t_{ma}}$ changes to the temperature of near-bottom seawater $\mathbf{t_{sf}}$ equal to −1.8°C at any part of the submerged shelf excluding locations near river mouths, which are influenced by river water plumes. Upon the regression, $\mathbf{t_{sf}}$ changes immediately to $\mathbf{t_{ma}}$ values typical of terrestrial conditions in a given time for a given latitude. It should be noted that reconstructed palaeo-temperature curves are more reliable for the Late Pleistocene and Holocene than for the earlier epochs. The absence of ice-bonded offshore permafrost within the shelf before 400 ka BP was taken as an initial condition. The vertical temperature gradient was calculated for a given type of geological section; this gradient was calculated for four different values of the geothermal heat flux $\mathbf{q_{gt}}$ (from 40 to 70 mW/m^2) characteristic of the undisturbed rock blocks in the rift zones.

4 GAS HYDRATE STABILITY ZONE SIMULATION

Along with simulation of permafrost evolution, the authors also simulated the dynamics of the gas hydrate stability zone (GHSZ) based on a model developed by G. Tipenko *et al.* (2001). According to this model, the groundwater pressure (P) is equal to the hydrostatic pressure at any depth. Sea transgression leads to the appearance of additional pressure (ΔP), equal to the pressure of the seawater column on the bottom. During transgressions, the groundwater pressure varied with the sea-level dynamics, whereas during regressions periods, it remained constant. The equality of groundwater pressure to the hydrostatic pressure was ensured by the presence of open subsea taliks along active tectonic faults and under the beds of palaeo-river valleys.

The modelling of GHSZ was based on the use of P/T diagrams developed by E. Chuvilin and E. Perlova (personal communication) for porous media and methane. The effect of groundwater salinity on the GHSZ was not taken into account because of the tentative character of the calculations. Calculations of the evolutionary dynamics of permafrost thickness and GHSZ were made for the geothermal heat flux value of 50 mW/m^2, which is typical of the shelf zone of both Laptev and East Siberian seas. The results of calculations were plotted on diagrams illustrating changes in the temperature field, the thickness of ice-bonded permafrost and boundaries of GHSZ typical of different depths of the sea and different latitudes (Fig. 2). Schematic maps of the thickness of ice-bonded offshore permafrost and the location of the lower boundary of the GHSZ were then compiled.

The modelling of permafrost evolution for rift zones was made for four climatic and glacio-eucstatic cycles and the range of $\mathbf{q_{gt}}$ values from 40 to 70 mW/m^2.

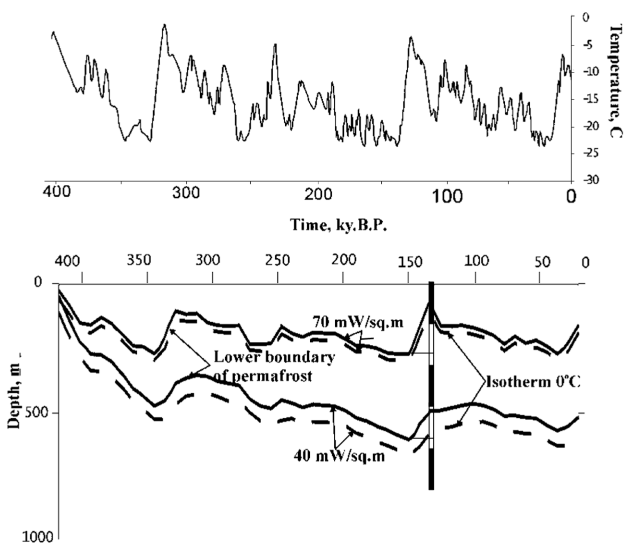

Figure 2. Example of dynamic of mean annual ground temperature (upper panel) and of permafrost lower boundary and isotherm 0°C (lower panel) during the last 400 kyr due to different values of geothermal flux. Yakutian coastal lowlands, latitude 71°N.

5 DISCUSSION OF MODELLING RESULTS

The results of modelling the thickness of ice-bonded offshore permafrost and the location of lower GHSZ boundary (for $\mathbf{q_{gt}}$ of 50 mW/m^2) are generalised on schematic maps. The simulation results show that the greatest thickness of ice-bonded offshore permafrost at the present time should exist in the area of New Siberian (Novosibirskie) Islands. There are vast shallows around these islands, where the duration of shelf exposure and permafrost aggradation were the longest, whereas the duration of submergence (during the last transgression) is relatively short.

The evolution of permafrost thickness under the impact of climate change within coastal lowlands and under the impact of transgressions and regressions within the shelf zone is characterised by a time lag ($-\Delta\tau$). The maximum thickness of ice-bonded permafrost is therefore reached with a time lag of several hundred to several thousand years, compared with the time of climatic minimums with the lowest $\mathbf{t_{ma}}$ values. In the phases of climate warming and sea transgressions, the maximum thawing (from the bottom) and minimum thickness of ice-bonded permafrost are attained later than the warming extreme (Fig. 2).

Simulation of the dynamics of permafrost thickness performed for different $\mathbf{q_{gt}}$ values (and mean annual temperatures $\mathbf{t_{ma}}$ and temperatures of bottom sediments $\mathbf{t_{sf}}$ below the thawing point) show that the maximum thickness of ice-bonded permafrost at the end of permafrost aggradation stages was generally inversely proportional to $\mathbf{q_{gt}}$ values. The rate of increase in permafrost thickness decreased by the end of permafrost aggradation stages. On the contrary, during the periods of climate warming (for coastal lowlands) and sea transgressions (for the shelf) accompanied by the rise in $\mathbf{t_{ma}}$ and $\mathbf{t_{sf}}$, the rates of permafrost thawing from the bottom first increased and then remained stable. Higher thawing rates corresponded to higher values of geothermal flux. As a result, the thickness of ice-bonded permafrost decreased in the periods of climatic warming and sea transgressions. This decrease was accompanied by spatial differentiation of permafrost thickness dictated by the difference of $\mathbf{q_{gt}}$ values within different lithospheric blocks. Taking into account the lag in time, this differentiation achieved its maximum during the initial phases of subsequent cooling on coastal lowlands and in the final phases of sea transgressions for the offshore permafrost (Fig. 3)

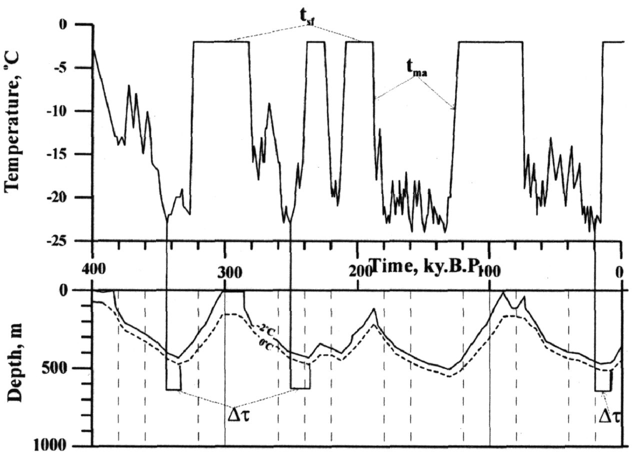

Figure 3. Delays of the maximal permafrost thickness relative to the climatic extremes (Δt). Upper panel – oscillation of the mean annual ground/bottom sediment temperature, lower panel – dynamics of the geothermal field. Laptev Sea Shelf, sea water depth −80 m, latitude 75°N, geothermal flux 50 mW/m^2.

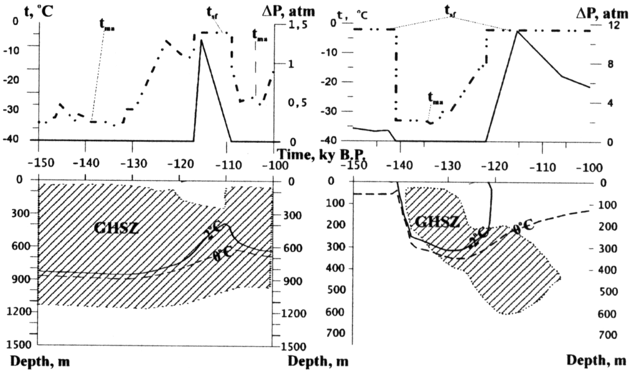

Figure 4. Dynamics of the upper boundary condition (temperature: $\mathbf{t_{ma}}/\mathbf{t_{sf}}$ and excess pressure-$\mathbf{\Delta P}$) and of gas hydrate stability zone (GHSZ) and geothermal field during the Kazantcevoan transgression on the Laptev Sea shelf. Left panel – sea depth −20 m, latitude 72°N, right panel – sea depth −100 m, latitude 77°N, geothermal heat flux 50 mW/m^2.

Two stages of changes in the temperature regime of offshore permafrost in the periods of transgression can be distinguished. At the first stage, after the submergence of the shelf and a sharp rise in temperature of the shelf surface (from $\mathbf{t_{ma}}$ to $\mathbf{t_{sf}} = -2.0$°C), a gradual levelling of temperatures within the whole thickness (from the top to the bottom) of ice-bonded permafrost takes place, so that the temperature gradient within the vertical profile of permafrost becomes equal to zero. This is accompanied by a gradual increase in the rate of thawing of ice-bonded permafrost. In the second stage, the thawing of ice-bonded permafrost from the bottom proceeds at a stable rate dictated by the geothermal flux value in a given area, the thermo-physical properties of the rocks, and the ice-content in them.

The zone of stability of methane hydrates appears on coastal lowlands simultaneously with the development of ice-bonded permafrost with a thickness of 300–400 m and then exists permanently during both cooling and warming climatic stages. The lower boundary of GHSZ is found 300 m below the lower boundary of the ice-bonded permafrost. Temporal variations in the depth of the lower boundary of GHSZ generally follows the same pattern as temporal variations in the depth of the lower boundary of ice-bonded permafrost (with a short lag period). These variations are controlled only by changes in the rock temperature, because hydrostatic pressure is assumed to be stable. The upper boundary of GHSZ lies within the thickness of ice-bonded permafrost. Its position (based on the modeling) is uncertain however, because the hydrostatic pressure of groundwater is not transferred within the thickness of ice-bonded permafrost.

The evolution of GHSZ within the shelf is different from that within coastal lowlands. During the stages of shelf drying, the thickness of ice-bonded permafrost and the position of its lower boundary are similar to those within coastal lowlands. However, during sea transgressions, the GHSZ position is controlled not only by the rise in temperature and lowering of the ice-bonded permafrost thickness but also by changes in the excess pressure $\mathbf{\Delta P}$ induced by fluctuations of sea level. In the inner shelf zone (with water depths less than 60 m) the GHSZ and ice-bonded permafrost do not disappear during transgression phases (Fig. 4). In the outer zone of shelf, both ice-bonded permafrost and GHSZ disappear completely by the end of transgressive phases. At the same time, at the beginning of transgressions, when the thickness of ice-bonded permafrost starts to decrease (owing to thawing from the bottom), the thickness of GHSZ remains stable or even increases owing to an increase in $\mathbf{\Delta P}$ during the transgression (Fig. 3). Figure 3 displays the results of modelling for the end of the Middle Pleistocene and beginning of the Late Pleistocene made for the isobaths of 20 and 100 m. Additional modelling (results not shown) suggests that, for a sea depth of 100 m and the geothermal flux value of 50 mW/m^2, the modern period is characterised by the end of thawing of ice-bonded permafrost and, at the same time, by a gradual increase in the thickness of the GHSZ (under the impact of excess hydrostatic pressure).

In the rift zones with $\mathbf{q_{gt}}$ of 50–60 mW/m^2 and the sea depths of less than 45–50 m, ice-bonded permafrost does not thaw completely during the stages of transgression. Ice-bonded permafrost is preserved and forms an impermeable (for groundwater and gases) layer. The disappearance of this layer is possible in the areas of deeper (>50 m) sea and/or higher $\mathbf{q_{gt}}$

values. The thawing of ice-bonded offshore permafrost may be accompanied by the disappearance of the GHSZ, which may lead to increasing emission of gases in the end of transgressive stages.

ACKNOWLEDGEMENTS

Research supported by the joint Russian-Germany "Laptev Sea System 2000" project & OSL, by RFBR (grant 00-05-64430) & US NSF Grant OPP 99-86826.

REFERENCES

Balobaev, V.T. (1991) Geothermal Conditions of North Asian Lithosphere in Permafrost Areas. Nauka Publisher: Novosibirsk. 193 p (in Russian)

Bauch, H.A., Mueller-Lupp, T., Taldenkova, E. et al. (2001) Chronology of the Holocene transgression at the North Siberian margin // *Global and Planetary Change*, No. 31, pp.125–139.

Chappel, J., Omura, A., McCulloch, M. et al. (1996) Reconciliation of Late Quaternary sea level derived from coral terraces at Huon Peninsula with deep-sea oxygen isotope records. *Earth and Planetary Science Letters*. pp. 227–236.

Danilov, I.D., Komarov, I.A., Vlasenko, A.Yu. (2000) Cryolithozone of East-Siberia shelf during the last 80 kyr. *Cryosphere of the Earth*, IV vol., No. 1, pp. 18–24. (in Russian)

Dmitrenko, I.A., Holemann, J., Kirilov, S.A. et al. (2001) Thermal regime at the Laptev Sea bottom layer and affecting processes. *Cryosphere of Earth*, V vol., No. 3, pp. 44–55. (in Russian)

Drachev, S.S., Savostin, L.A., Bruni, J.E. (1995) Structural pattern and tectonic history of the Laptev Sea Region. *Reports of Polar Research* 176. pp. 348–367.

Fairbanks, R. (1989) A 17.000-year glacio-eustatic sea level record: Influence of glacial melting rates on the Younger Dryas event and deep ocean circulation. *NATURE*, No. 342, pp. 636–642.

Fartyshev, A.I. (1993) Peculiarities of Near Shore and Shelf Cryolithozone of Laptev Sea Shelf. Novosibirsk, NAUKA Publisher. 135 p. (in Russian)

Gavrilov, A.V., Tumskoy, V.E. (2000) The Evolution of the Mean annual Ground Temperature on Coastal Lowlands in Middle and Late Pleistocene. *Cryosphere of Earth*, IV vol., No. 3, pp. 3–16. (in Russian)

Gavrilov, A.V., Tumskoy, V.E., Romanovskii, N.N. (2000) Reconstruction of the mean annual ground temperature dynamic on the Yacutian coastal lowlands and adjoining shelf during the last 400 ky. *Cryosphere of Earth*, IV vol., No. 4, pp. 3–14. (in Russian)

Geocryology of USSR. East Siberia and Far East. (1989) NEDRA Publisher. Moscow. 515 p. (in Russian)

Kholodov, A.L., Gavrilov, A.V., Romanovskii, N.N., Hubberten, H.W. (2000) Results of modeling of permafrost dynamic on Arctic shelf and coastal lowlands in the Laptev sea region during the last 400 ky. *Cryosphere of the Earth*, IV vol, No. 4 pp. 32–40.

Lysak, S.V. (1988) Geothermal Heat Flux of Continental Rifts. NAUKA Publisher: Moscow. 213 p. (in Russian)

Petit, J.R., Jouzel, J., Raynaud, D. et al. (1999) Climate and atmospheric history of the past 420 000 years from the Vostok ice core, Antarctica. *NATURE*, vol. 399, pp. 429–436.

Romanovskii, N.N., Gavrilov, A.V., Kholodov, A.L. et al. (1998) The Forecasting Map of Laptev Sea Shelf Offshore Permafrost. *"Proceedings of the Seventh Permafrost International Conference"*. Yellowknife, Canada. Vol. 1. pp. 967–972.

Romanovskii, N.N., Hubberten, H.-W. (2001) Results of Permafrost Modelling of the Lowlands and Shelf of Laptev Sea Region, Russia. *Permafrost and Periglacial Processes*, 12: 191–202.

Romanovskii, N.N., Gavrilov, A.V., Tumskoy, V.E., Kholodov, A.L., Siegert, Ch. Hubberten H.-W., Sher, A. (2000) Environmental Evolution in the Laptev Sea Region During Late Pleistocene and Holocene. *Polarforschung* 68, pp. 237–245.

Romanovskii, N.N., Hubberten, H.-W., Kholodov, A.L., Tipenko, G.S. (2001) Offshore Permafrost State on the Shelf on the Eastern Sector Russian arctic Seas. *Cryosphere of Earth*, V vol, No. 2, pp. 3–10. (in Russian)

Soloviev, V. A. (1981) Prediction of the distribution of relict subaqual frozen zone (on the example of Arctic seas). Developmental regularities of the cryolithozone in the Arctic basin. // *The Cryolithozone of the Arctic Shelf*. Yakutsk: 28–38. (in Russian)

Tectonic Map of Kare and Laptev Seas (scale 1: 2.500 000). Explanation note (1998). Moscow. 127 p. (in Russian)

Tipenko, G.S., Romanovskii, N.N., Kholodov, A.L. (2001) Simulation of the Offshore Permafrost and Gas hydrate Stability Zone: mathematical solution, Numerical realisation and preliminary results. *Polarforshung* 69, pp. 229–227.

Zhigarev, L.A. (1997) *The Oceanic Cryolithozone*. Moscow State University Publisher 318 p (in Russian)